Application of the velocity-dissipation probability density function model to inhomogeneous turbulent flows

S. B. Pope
Sibley School of Mechanical and Aerospace Engineering, Cornell University, Ithaca, New York 14853

(Received 20 February 1991; accepted 17 April 1991)

Recently Pope and Chen [Phys. Fluids A **2**, 1437 (1990)] developed a turbulence model based on the one-point Eulerian joint probability density function (pdf) of velocity and dissipation. The modeling is performed by constructing stochastic processes for the velocity and dissipation following fluid particles. In the original work, these models were constructed by reference to the known statistics of homogenous turbulence, and the applicability of the model was restricted to this narrow class of flows. In this paper the model is extended to inhomogeneous flows, and calculations are presented to demonstrate aspects of the model's performance. The model equation admits a similarity solution corresponding to the log-law region of the turbulent boundary layer, and the principal statistics obtained from this solution are in good agreement with experimental data. Application of the model to the momentumless wake and to the plane mixing layer demonstrate its ability to represent turbulent/nonturbulent intermittency in these free flows: in the intermittent regions, the pdf of dissipation is bimodal, with a spike at zero corresponding to nonturbulent fluid. Fluid-particle paths in the turbulent mixing layer obtained from the model correspond to large-scale coherent motions, rather than to the small-scale incoherent motion characteristic of diffusive transport.

I. INTRODUCTION

There is a continuing need for turbulence models capable of calculating the inhomogeneous turbulent flows that occur in engineering equipment and elsewhere.[1,2] Most models in current use are one-point closures, such as the k-ϵ model,[3,4] or Reynolds-stress models.[5-7] In spite of some of the sophisticated modeling techniques that have been developed, it should be recognized that at each point in a complex inhomogeneous turbulent flow, these models characterize the state of the turbulence by just a few numbers—by the values of k and ϵ, or by the six Reynolds stresses and ϵ. And at some level, turbulent transport is modeled as gradient diffusion.

Probability density function (pdf) methods[8] offer the possibility of a much more comprehensive description of the turbulence, and the complete avoidance of gradient-diffusion modeling, while still being tractable computationally. Recent applications of pdf methods (reviewed by Pope[2]) include calculations of two-dimensional recirculating flows,[9,10] and calculations of the two- and three-dimensional time-dependent flow in spark-ignition engines.[11,12]

Until recently, the most comprehensive pdf model has been based on the one-point Eulerian joint pdf of velocity and composition.[13,8] While this pdf describes the distribution of velocities, its description of the turbulent motions is seriously deficient, in that it provides no information on their length or time scales. To remedy this deficiency, Pope and Chen[14] recently developed a model based on the joint pdf of velocity and (the instantaneous) dissipation rate. This model was developed by reference to the known statistics of homogeneous turbulence, and in its original form it is restricted to homogeneous turbulence. In this paper the model is extended to the general case of inhomogeneous flows, and calculations are made to demonstrate its performance.

As is in previous pdf studies,[2,8,13,14] we adopt the Lagrangian view in performing the modeling. Specifically, we construct stochastic models [$\mathbf{U}^*(t)$ and $\epsilon^*(t)$] for the velocity and dissipation following a fluid particle. By definition, the position of the fluid particle $\mathbf{x}^*(t)$ moves with the velocity $\mathbf{U}^*(t)$; while (by assumption) $\mathbf{U}^*(t)$ and $\epsilon^*(t)$ evolve according to coupled diffusion processes.[8,15]

These stochastic models lead to an evolution equation for the one-point Eulerian joint pdf of velocity and dissipation. This procedure effects a closure, since the coefficients in the joint pdf equation are Eulerian statistics of velocity and dissipation that can be deduced from the joint pdf itself. And the coefficients in the diffusion processes for $\mathbf{U}^*(t)$ and $\epsilon^*(t)$ are functions of $\mathbf{U}^*(t)$, $\epsilon^*(t)$, and Eulerian statistics evaluated at $\mathbf{x}^*(t)$.

In Secs. II and III the stochastic models for $\epsilon^*(t)$ and $\mathbf{U}^*(t)$ are extended to inhomogeneous flows, and the corresponding joint pdf equation is presented in Sec. IV. Calculations are presented in Sec. V for three flows: the log-law region of the turbulent boundary layer; the momentumless wake; and the plane mixing layer. The results demonstrate the quantitative accuracy of the model in strongly inhomogeneous flows, including its ability to represent realistically turbulent/nonturbulent intermittent regions.

The development of turbulence models involves many decisions—in particular, about the forms of constitutive relations. In making these decisions, the overriding criterion used here is simplicity. At the given level of closure, the model is designed to be as simple as possible, while being qualitatively correct and quantitatively reasonable. The model is aimed at moderate and high Reynolds number flows, but contains no Reynolds number dependence. There is no doubt that there is scope for improving the accuracy and generality of the modeling, including the incorporation of Reynolds number effects. But such improvements are best

 0899-8213/91/081947-11$02.00

made in the light of experience with the basic model presented here.

II. STOCHASTIC MODEL FOR DISSIPATION

A. Definitions

We consider the turbulent flow of a Newtonian fluid of constant density ρ and kinematic viscosity ν. At position $\mathbf{x}$ and time t, the Eulerian velocity is $\mathbf{U}(\mathbf{x},t)$ with mean (or mathematical expectation) $\langle \mathbf{U}(\mathbf{x},t)\rangle$ and fluctuation $\mathbf{u}(\mathbf{x},t)$,

$$\mathbf{U}(\mathbf{x},t) = \langle \mathbf{U}(\mathbf{x},t)\rangle + \mathbf{u}(\mathbf{x},t). \tag{1}$$

The turbulent kinetic energy is

$$k(\mathbf{x},t) = \tfrac{1}{2}\langle \mathbf{u}(\mathbf{x},t)\cdot\mathbf{u}(\mathbf{x},t)\rangle. \tag{2}$$

For reasons given by Pope and Chen,[14] rather than the true dissipation, we consider the pseudodissipation defined by

$$\epsilon(\mathbf{x},t) \equiv \nu\left\langle \frac{\partial u_i}{\partial x_j}\frac{\partial u_i}{\partial x_j}\right\rangle, \tag{3}$$

which henceforth is referred to as "dissipation."

For the development that follows, it is convenient to define dissipation-weighted means, which are denoted by a tilde; for example,

$$\tilde{\mathbf{U}}(x,t) \equiv \langle \mathbf{U}(\mathbf{x},t)\epsilon(\mathbf{x},t)\rangle / \langle \epsilon(\mathbf{x},t)\rangle \tag{4}$$

and

$$\tilde{k}(\mathbf{x},t) \equiv \tfrac{1}{2}\langle \mathbf{u}\cdot\mathbf{u}\epsilon\rangle / \langle\epsilon\rangle. \tag{5}$$

Note that, in Eq. (5), the regular fluctuation $\mathbf{u}$ is used, rather than $\tilde{\mathbf{u}} \equiv \mathbf{U} - \tilde{\mathbf{U}}$.

For homogeneous turbulence, the model of Pope and Chen[14] yields a joint-normal solution: specifically the one-point, one-time Eulerian joint pdf of $\mathbf{U}$ and $\ln\epsilon$ is joint normal, with $\ln\epsilon$ being uncorrelated with $\mathbf{U}$. We refer to this solution as pertaining to *Gaussian homogeneous turbulence* (GHT), and we require the model developed here to revert to GHT in the appropriate circumstances.

In GHT $\epsilon(\mathbf{x},t)$ is independent of $\mathbf{u}(\mathbf{x},t)$ (because $\mathbf{U}$ and $\ln\epsilon$ are uncorrelated and joint normal). Hence dissipation-weighted and regular velocity statistics are the same. For example, we have

$$\tilde{k}(\mathbf{x},t) \overset{G}{=} k(\mathbf{x},t), \tag{6}$$

where $\overset{G}{=}$ denotes equality for Gaussian homogeneous turbulence.

The position, velocity, and dissipation of a fluid particle are denoted by $\mathbf{x}^+(t)$, $\mathbf{U}^+(t)$, $\epsilon^+(t)$, and similarly for any other property. By definition, the position evolves by

$$\frac{d\mathbf{x}^+(t)}{dt} = \mathbf{U}^+(t), \tag{7}$$

while the relationship between other Lagrangian quantities and the Eulerian fields is, for example,

$$\epsilon^+(t) = \epsilon(\mathbf{x}^+[t],t). \tag{8}$$

The stochastic models to be developed, $\mathbf{U}^*(t)$ and $\epsilon^*(t)$, are models for the corresponding Lagrangian properties $\mathbf{U}^+(t)$ and $\epsilon^+(t)$. The modeled particle's position $\mathbf{x}^*(t)$ then evolves by

$$\frac{dx^*(t)}{dt} = \mathbf{U}^*(t). \tag{9}$$

B. Relaxation rate

The *relaxation rate* $\omega(\mathbf{x},t)$ is defined by

$$\omega(\mathbf{x},t) = \epsilon(\mathbf{x},t)/\tilde{k}(\mathbf{x},t), \tag{10}$$

which is a mixed variable in the sense that ϵ is random, whereas $\tilde{k}$ is not. As in Pope and Chen[14] we use $\omega(\mathbf{x},t)$ as a primary variable rather than $\epsilon(\mathbf{x},t)$. The main reason is that (on dimensional grounds) it is possible to write a model evolution equation for ω^* solely in terms of ω^* itself: $d\omega^*/dt$ has the same dimensions as ω^{*2} (or $\langle\omega\rangle^2$). On the other hand, an evolution equation for ϵ must also involve statistics of $\mathbf{u}$: $d\epsilon^*/dt$ has dimensions of ϵ^{*2}/k.

The use of $\tilde{k}$ rather than k in the definition of ω [Eq. (10)] has a purely pragmatic justification. In intermittent regions—such as the edge of free shear flows—$\tilde{k}$ is considerably larger than k. Consequently, for given $\langle\omega\rangle$, Eq. (10) yields greater mean dissipation ($\langle\epsilon\rangle = \langle\omega\rangle\tilde{k}$) than if the unweighted kinetic energy were used. It is found that this enhanced dissipation significantly improves the model's performance.

It may be seen from Eqs. (4) and (10) that ω-weighted means are identical to ϵ-weighted means.

C. Model for Gaussian homogeneous turbulence

We review now the model for $\omega^*(t)$ developed by Pope and Chen[14] for GHT.

The relaxation rate $\omega^*(t)$ evolves according to the Ito stochastic differential equation[15]

$$d\omega^* = -\omega^*\langle\omega\rangle dt\{S_\omega + C_\chi[\ln(\omega^*/\langle\omega\rangle) - \tfrac{1}{2}\sigma^2]\} + \omega^*(2C_\chi\langle\omega\rangle\sigma^2)^{1/2}\,dW, \tag{11}$$

where $W(t)$ is a Wiener process. This equation is perhaps best understood in terms of the statistical properties of $\omega^*(t)$ that it produces, or in terms of the statistics of

$$\chi^*(t) \equiv \ln[\omega^*(t)/\langle\omega(t)\rangle]. \tag{12}$$

Equation (11) implies that $\chi^*(t)$ is an Ornstein–Uhlenbeck process[15] with mean $-\tfrac{1}{2}\sigma^2$, variance σ^2, and time scale

$$T_\chi = [C_\chi\langle\omega\rangle]^{-1}. \tag{13}$$

That is, $\chi^*(t)$ is a Gaussian process with autocorrelation function $\exp(-|t|/T_\chi)$. Thus $\omega^*(t)$ is lognormally distributed. For the mean, Eq. (11) yields

$$\frac{d\langle\omega\rangle}{dt} = -\langle\omega\rangle^2 S_\omega. \tag{14}$$

The coefficients in Eq. (11) have now been identified: σ^2 is the variance of $\ln\omega^*$; C_χ is a proportionality constant between the time scale T_χ and $\langle\omega\rangle^{-1}$; and S_ω is the normalized decay rate of $\langle\omega\rangle$. For reasons given by Pope and Chen,[14] the values $\sigma^2 = 1.0$ and $C_\chi = 1.6$ are specified. A specification of S_ω that is consistent with the standard model equation[3,4] for $\langle\epsilon\rangle$ is

$$S_\omega = (C_{\epsilon 2} - 1) - (C_{\epsilon 1} - 1)P/\langle\epsilon\rangle, \tag{15}$$

where P is the production rate of k, and $C_{\epsilon 1}$ and $C_{\epsilon 2}$ are standard model constants.

D. Model for inhomogeneous flows

The model stochastic differential equation for $\omega^*(t)$ applicable to inhomogeneous flows is first presented, and then contrasted to Eq. (11). The equation is

$$d\omega^* = -\omega^*\langle\omega\rangle dt \times\left\{S_\omega + C_\chi\left[\ln\left(\frac{\omega^*}{\langle\omega\rangle}\right) - \left\langle\frac{\omega}{\langle\omega\rangle}\ln\left(\frac{\omega}{\langle\omega\rangle}\right)\right\rangle\right]\right\} + \langle\omega\rangle^2 h\, dt + \omega^*(2C_\chi\langle\omega\rangle\sigma^2)^{1/2}\, dW. \tag{16}$$

Note that means [e.g., $\langle\omega(\mathbf{x},t)\rangle$] and coefficients [e.g., $h(x,t)$] depend on both position and time.

Comparing Eq. (16) to Eq. (11), it may be seen that the diffusion coefficient (that multiplies dW) is unchanged. In the drift coefficient, $\frac{1}{2}\sigma^2$ [in Eq. (11)] has been replaced by

$$\left\langle\frac{\omega}{\langle\omega\rangle}\ln\left(\frac{\omega}{\langle\omega\rangle}\right)\right\rangle \overset{G}{=} \frac{1}{2}\sigma^2. \tag{17}$$

This is done so that, in the equation for the mean $\langle\omega\rangle$, the terms in C_χ vanish, irrespective of the distribution of $\omega^*(t)$.

If the expression for the production P given by the k-ϵ model[3,4] is substituted into Eq. (15), the result is

$$S_\omega = -C_{\omega 1}S_{ij}S_{ij}/\langle\omega\rangle^2 + C_{\omega 2}, \tag{18}$$

where S_{ij} is the mean rate of strain:

$$S_{ij} \equiv \frac{1}{2}\left(\frac{\partial\langle U_i\rangle}{\partial x_j} + \frac{\partial\langle U_j\rangle}{\partial x_i}\right), \tag{19}$$

and the constants $C_{\omega 1}$ and $C_{\omega 2}$ are related to the k-ϵ model constants by

$$C_{\omega 1} = 2C_\mu(C_{\epsilon 1} - 1) \tag{20}$$

and

$$C_{\omega 2} = C_{\epsilon 2} - 1. \tag{21}$$

We use Eq. (18) to specify S_ω, with $C_{\omega 2} = 0.9$ (consistent with the standard value $C_{\epsilon 2} = 1.9$), and $C_{\omega 1} = 0.04$, which is significantly less than the value 0.081, consistent with $C_\mu = 0.09$ and $C_{\epsilon 1} = 1.45$. The choice of $C_{\omega 1}$ is discussed in Sec. V.

For several reasons, the specification of S_ω is regarded as being provisional. First, a combination of the mean rate of strain and the mean rotation may be more appropriate.[6] Second, the expression [Eq. (18)] involves ω^* only through its mean. Since at this level of closure the distribution of ω^* is known, it is likely that more of this information could be used to produce a more accurate constitutive relation for S_ω.

For Gaussian homogeneous turbulence, $\omega^*(t)$ is lognormally distributed, and hence there is zero probability of $\omega^*(t)$ being zero. For inhomogeneous flows, however, this is not the case, and the behavior of the model for $\omega^*(t) = 0$ needs careful consideration—and, it transpires, the introduction of the term in h in Eq. (16).

Consider, for example, a fluid particle that is initially remote from a turbulent jet issuing into nominally quiescent surroundings. At first, the particle moves with the slow, irrotational flow induced by the jet. The fluctuations (in velocity, strain rate, etc.) are initially very small, but increase as the particle nears the jet.[16] The particle is then entrained and becomes part of the fully turbulent motion within the jet.

Remote from the turbulent jet $\langle\omega(\mathbf{x},t)\rangle$ is zero. This cannot be deduced from the definition $\langle\omega\rangle \equiv \langle\epsilon\rangle/\tilde{k}$, since both $\langle\epsilon\rangle$ and $\tilde{k}$ tend to zero with distance from the jet. But experimental data (see, e.g., Townsend[17]) and theory[16,18] both indicate that $\langle\epsilon\rangle$ decreases with distance from the jet more rapidly than does $\tilde{k}$. Thus the fluid particle considered starts with the value $\omega^* = 0$, which increases to a strictly positive value as the particle is entrained into the turbulent flow.

With this particle in mind, we examine now the behavior of Eq. (16) (with $h = 0$) with the initial condition $\omega^* = 0$. The first observations is that the equation is well defined, since $\ln\omega^*$ only appears as $\omega^*\ln\omega^*$ (which is finite for all finite $\omega^* \geqslant 0$). Second, with the initial condition $\omega^* = 0$, the solution to Eq. (16) (with $h = 0$) is that ω^* remains zero for all time. It is clear, then, that a modification to the model for ω^* is needed to provide a mechanism by which ω^* can depart from zero as the particle is entrained into the turbulent flow.

Two types of modifications are possible: a jump process could be added; or an additional drift term could be included in Eq. (16). Physical arguments can be mustered for both options, but our detailed knowledge of the entrainment process is insufficient to provide clear judgment between them. For simplicity, and to retain continuous sample paths $\omega^*(t)$, we choose the latter option, and add the drift term in h to Eq. (16).

The additional drift coefficient H, say, [i.e., $h\langle\omega\rangle^2$ in Eq. (16)] is required to satisfy the following conditions:

(1) $H = 0$ for Gaussian homogeneous turbulence (so the model reverts to that of Pope and Chen in GHT) [the requirement $H = 0$ is so that the lognormal solution for ω^* is recovered for GHT. But in fact, we require more: we require that the form of H does not make this solution unstable. See the discussion above Eq. (26)];

(2) $H = 0$ for $\langle\omega\rangle = 0$ (so that ω^* remains zero in a region of fully nonturbulent fluid); and

(3) $H > 0$ for $\omega^* = 0$ and $\langle\omega\rangle > 0$ in non-GHT (so that ω^* increases from zero in intermittent regions).

These conditions are satisfied by the chosen form

$$H = \langle\omega\rangle^2 h, \tag{22}$$

where h is a non-negative mean quantity [independent of $\omega^*(t)$] that is zero in GHT.

The specification of h is based on the fractional moment

$$\mu_{1/2} \equiv \langle\omega^{1/2}\rangle/\langle\omega\rangle^{1/2}, \tag{23}$$

which is bounded by zero and unity, and for Gaussian homogeneous turbulence takes the value

$$\mu_{1/2} \overset{G}{=} \mu_{1/2G} = e^{-\sigma^2/8}. \tag{24}$$

(With $\sigma^2 = 1$, $\mu_{1/2G} \approx 0.8825$.)

To illustrate the significance of $\mu_{1/2}$, we consider a region of turbulent/nonturbulent flow with intermittency factor γ. Suppose that ω^* is zero with probability $(1-\gamma)$, and that it is lognormally distributed (with parameter σ^2) with

probability γ. Then it is readily shown that

$$\mu_{1/2} = \gamma^{1/2}\mu_{1/2G}. \tag{25}$$

In general, then, we expect that in intermittent regions $\mu_{1/2}$ is less than $\mu_{1/2G}$, and that it tends to zero as a fully nonturbulent state is approached. The numerical calculations reported below confirm this expectation.

Nevertheless, we need to consider the case $\mu_{1/2} > \mu_{1/2G}$. An effect of the term in h (for $h > 0$) is to increase $\mu_{1/2}$ as time evolves. Thus if h is positive for $\mu_{1/2} > \mu_{1/2G}$, the effect of the term is to drive the distribution yet farther away from the GHT solution. In other words, the term makes the GHT solution unstable. To avoid this difficulty we simply specify

$$h = 0, \quad \text{for } \mu_{1/2} > \mu_{1/2G}. \tag{26}$$

And for the usual case we specify

$$h = C_{\omega 3}(1 - \mu_{1/2}/\mu_{1/2G})^2, \quad \text{for } \mu_{1/2} \leqslant \mu_{1/2G}, \tag{27}$$

with $C_{\omega 3} = 1$. In Eq. (27) the expression in brackets (which is zero in GHT) is squared, first, to make h once continuously differentiable with respect to $\mu_{1/2}$; and, second, to reduce the influence of the term near the GHT limit.

While comprehensive systematic testing has not been performed, it nevertheless appears that the calculations reported below are insensitive to the precise specification of h, including the value of $C_{\omega 3}$.

Finally, we mention an implicit assumption that has been made. The equation for $\omega^*(t)$ applicable to inhomogeneous flows has been developed simply by extending the model for GHT with a minimum of modification. In particular, no terms in ∇k or $\nabla\langle\omega\rangle$ have been added. An alternative approach would be to extend the model for $\epsilon^*(t)$, and then to use the definition of $\omega^*(t)$ [Eq. (10)] to derive the corresponding model for $\omega^*(t)$. This latter approach would, in comparison to Eq. (16), produce an additional term of the form

$$d\omega^* = \cdots - \omega^*\, dt\, \mathbf{u}^*\cdot\nabla \ln \tilde{k} \cdots. \tag{28}$$

Since we do not include such a term, we are implicitly assuming that (in the absence of all other effects) ω^*, rather than ϵ^*, is conserved as the fluid particle moves through an inhomogeneous $\tilde{k}$ field.

In summary: for inhomogeneous flows, $\omega^*(t)$ evolves by the stochastic differential equation, Eq. (16), with S_ω given by Eq. (18), and H given by Eqs. (26) and (27). The values of the constants are $\sigma^2 = 1.0$, $C_\chi = 1.6$, $C_{\omega 1} = 0.04$, $C_{\omega 2} = 0.9$, and $C_{\omega 3} = 1.0$. For Gaussian homogeneous turbulence the model reverts to that of Pope and Chen,[14] according to which $\omega^*(t)$ is lognormally distributed, and $\chi^*(t) \equiv \ln[\omega^*(t)/\langle\omega\rangle]$ is an Ornstein–Uhlenbeck process with variance σ^2 and time scale $T_\chi = [C_\chi\langle\omega\rangle]^{-1}$. The principal modification required for inhomogeneous turbulence is the addition of the drift term in h, which allows $\omega^*(t)$ to increase from zero.

III. STOCHASTIC MODEL FOR VELOCITY

A. General form

We now develop a stochastic model $\mathbf{U}^*(t)$ for the velocity $\mathbf{U}^+(t)$ following a fluid particle. Both the stochastic model of Pope and Chen,[14] and the generalization developed here can be written as

$$dU_i^* = -\frac{1}{\rho}\frac{\partial\langle p\rangle}{\partial x_i}\,dt + D_i\,dt + (C_0\epsilon^*)^{1/2}\,dW_i, \tag{29}$$

where D_i is the drift coefficient (discussed below), C_0 is a constant (ascribed the value $C_0 = 3.5$), and $\mathbf{W}(t)$ is an isotropic Wiener process, with the properties

$$\langle dW_i\rangle = 0, \quad \langle dW_i\, dW_j\rangle = dt\,\delta_{ij}. \tag{30}$$

Assuming that the mean viscous force $\rho\nu\nabla^2\langle\mathbf{U}\rangle$ is negligible, conservation of mean momentum requires

$$\langle dU_i^*\rangle = -\frac{1}{\rho}\frac{\partial\langle p\rangle}{\partial x_i}\,dt, \tag{31}$$

which in turn requires that the drift coefficient be constrained by

$$\langle D_i\rangle = 0. \tag{32}$$

The diffusion term (involving $\epsilon^* = \tilde{k}\omega^*$) models the fluid-particle acceleration on the smallest time scales. With the assumed local isotropy at high Reynolds number, the model developed for Gaussian homogeneous turbulence is applicable to inhomogeneous flows.

B. Model for Gaussian homogeneous turbulence

With the diffusion term unaltered, the development centers on the drift term D_i. The extension of the model to inhomogeneous flows is performed by requiring that certain basic properties be preserved. These properties are described in this section.

For Gaussian homogeneous turbulence, the primary effect of the drift term D_i is seen in the corresponding Reynolds-stress equation. From Eq. (29) (for GHT) we obtain

$$\frac{d}{dt}\langle u_i u_j\rangle + \langle u_i u_l\rangle\frac{\partial\langle U_j\rangle}{\partial x_l} + \langle u_j u_l\rangle\frac{\partial\langle U_i\rangle}{\partial x_l} = R_{ij}, \tag{33}$$

where

$$R_{ij} = \langle D_i u_j\rangle + \langle D_j u_i\rangle + C_0\langle\epsilon\rangle\delta_{ij}. \tag{34}$$

The terms on the left-hand side of Eq. (33) represent the time rate of change and production. The terms on the right-hand side of Eq. (34) model the effects of the pressure-rate-of-strain and dissipation. Thus R_{ij} corresponds to the modeled terms in a Reynolds-stress closure.

For GHT the model of Pope and Chen[14] is

$$\begin{aligned} D_i &= D_i^{(1)} + D_i^{(2)} + D_i^{(3)} \\ &= -(\tfrac{1}{2} + \tfrac{3}{4}C_0)\langle\omega\rangle u_i^* + G_{ij}^a u_j^* \\ &\quad - \tfrac{3}{4}C_0(\omega^* - \langle\omega\rangle)A_{ij}^{-1}u_j^*, \end{aligned} \tag{35}$$

where $D_i^{(1)}$, $D_i^{(2)}$, and $D_i^{(3)}$ are defined by the three terms on the second line of the equation. Here $\mathbf{u}^*$ is the fluctuation relative to the local Eulerian mean:

$$\mathbf{u}^*(t) \equiv \mathbf{U}^*(t) - \langle\mathbf{U}(\mathbf{x}^*(t),t)\rangle, \tag{36}$$

and G_{ij}^a and A_{ij}^{-1} are defined below. The contributions to R_{ij} made by $D_i^{(1)}$, $D_i^{(2)}$ and $D_i^{(3)}$ are now determined.

We define $R_{ij}^{(1)}$ to be the contribution to R_{ij} from $D_i^{(1)}$, and from the diffusion term

$$R_{ij}^{(1)} \equiv \langle D_i^{(1)} u_j \rangle + \langle D_j^{(1)} u_i \rangle + C_0 \langle \epsilon \rangle \delta_{ij}. \tag{37}$$

Substituting $D_i^{(1)}$ from Eq. (35) we obtain

$$\begin{aligned} R_{ij}^{(1)} &= -(1 + \tfrac{3}{2}C_0)\langle \omega \rangle \langle u_i u_j \rangle + C_0 \langle \epsilon \rangle \delta_{ij} \\ &= -(1 + \tfrac{3}{2}C_0)\langle \omega \rangle (\langle u_i u_j \rangle - \tfrac{2}{3}k\delta_{ij}) - \tfrac{2}{3}\langle \epsilon \rangle \delta_{ij}. \end{aligned} \tag{38}$$

It may be seen, then, that this corresponds to isotropic dissipation ($-\frac{2}{3}\langle \epsilon \rangle \delta_{ij}$), plus Rotta's return to isotropy model.[19]

On contracting Eq. (38) to obtain the trace $R_{ii}^{(1)}$, the Rotta term vanishes, leaving

$$\tfrac{1}{2}R_{ii}^{(1)} = -\langle \epsilon \rangle. \tag{39}$$

The second contribution to the Reynolds-stress evolution is

$$R_{ij}^{(2)} \equiv G_{il}^a \langle u_j u_l \rangle + G_{jl}^a \langle u_i u_l \rangle. \tag{40}$$

In general, G_{ij}^a is a second-order tensor function of the Reynolds stresses and mean velocity gradients, constrained by the requirement

$$\tfrac{1}{2}R_{ii}^{(2)} = G_{ij}^a \langle u_i u_j \rangle = 0. \tag{41}$$

In the calculations presented below we take G_{ij}^a to be zero, so that the corresponding Reynolds-stress equation [Eq. (33)] is just Rotta's model. Alternatively, there is a choice of G_{ij}^a corresponding to any (realizable) Reynolds-stress model. A specific form is given by Haworth and Pope.[20,21]

In the third contribution $D_i^{(3)}$ [Eq. (35)] A_{ij} is the normalized Reynolds-stress tensor

$$\begin{aligned} A_{ij} &\equiv \langle u_i u_j \rangle / (\tfrac{2}{3}k), \\ &= 3\langle u_i u_j \rangle / \langle u_l u_l \rangle, \end{aligned} \tag{42}$$

normalized so that in isotropic turbulence it is the identity $A_{ij} = \delta_{ij}$. Then A_{ij}^{-1} is written for $(\mathbf{A}^{-1})_{ij}$, i.e., the $i-j$ component of the inverse of $\mathbf{A}$. The term makes no contribution to the Reynolds-stress evolution since (in GHT)

$$R_{ij}^{(3)} \equiv \langle D_i^{(3)} u_j \rangle + \langle D_j^{(3)} u_i \rangle = 0. \tag{43}$$

(This follows from $\langle \omega u_i u_j \rangle \overset{G}{=} \langle \omega \rangle \langle u_i u_j \rangle$.) Even though it has no direct effect on $\langle u_i u_j \rangle$, the term in A_{ij}^{-1} is nevertheless necessary to yield the required joint normality of $\mathbf{u}^*(t)$ (in GHT).[14]

Finally, we observe that the exact evolution equation for the kinetic energy $k = \frac{1}{2}\langle u_i u_i \rangle$ requires

$$\tfrac{1}{2}R_{ii} = -\langle \epsilon \rangle. \tag{44}$$

Since the traces $R_{ii}^{(2)}$ and $R_{ii}^{(3)}$ are zero [Eqs. (41) and (43)], this requirement [Eq. (44)] is satisfied by $R_{ii}^{(1)}$ [Eq. (39)].

C. Model for inhomogeneous flows

In extending the model to inhomogeneous flows, no additional terms are introduced. The existing terms contributing to D_i [Eq. (35)] are modified to preserve the following properties: (1) $\langle D_i \rangle = 0$ (for consistency with mean momentum conservation); (2) $R_{ij}^{(1)}$ [Eq. (37)] corresponds to isotropic dissipation plus Rotta's model [i.e., Eq. (38)]; (3) $R_{ij}^{(2)}$ is given by Eq. (40); and (4) and $R_{ij}^{(3)}$ [Eq. (43)] is zero.

Modifications are needed because for GHT the above properties follow from the definition of D_i [Eq. (35)], only because $\mathbf{u}^*$ and ω^* are statistically independent. For the inhomogeneous case, on the other hand, $\langle \mathbf{u}\omega \rangle$ is nonzero (in general), and the normalized Reynolds-stress tensor A_{ij} [Eq. (42)] differs from its ω-weighted counterpart

$$\begin{aligned} \tilde{A}_{ij} &\equiv \langle \omega u_i u_j \rangle / (\tfrac{2}{3}\langle \omega \rangle \tilde{k}) \\ &= 3\langle \omega u_i u_j \rangle / \langle \omega u_l u_l \rangle. \end{aligned} \tag{45}$$

The modified drift term, which has the four required properties, is

$$\begin{aligned} D_i = &-(\tfrac{1}{2} + \tfrac{3}{4}C_0)\langle \omega \rangle (\tilde{k}/k) u_i^* + G_{ij}^a u_j^* \\ &- \tfrac{3}{4}C_0 [(k/\tilde{k})\tilde{A}_{ij}^{-1}(\omega^* u_j^* - \langle \omega u_j \rangle) \\ &- A_{ij}^{-1}\langle \omega \rangle u_j^*]. \end{aligned} \tag{46}$$

In the first term ($D_i^{(1)}$), the inclusion of the kinetic energy ratio is necessary so that, as in GHT,

$$\langle \omega \rangle \tilde{k}/k = \langle \epsilon \rangle / k. \tag{47}$$

The second term ($D_i^{(2)}$) involving G_{ij}^a is unaltered.

The third term ($D_i^{(3)}$) suffers more substantial modification. The mean $\langle \omega u_j \rangle$ is subtracted to maintain $\langle D_i \rangle = 0$. In forming $R_{ij}^{(3)}$ (which is zero), one contribution is

$$\begin{aligned} \langle u_j (A_{il}^{-1}\langle \omega \rangle u_l) \rangle &= \langle \omega \rangle A_{il}^{-1} \langle u_l u_j \rangle \\ &= \tfrac{2}{3}k \langle \omega \rangle A_{il}^{-1} A_{lj} \\ &= \tfrac{2}{3}k \langle \omega \rangle \delta_{ij}. \end{aligned} \tag{48}$$

The term in $\tilde{A}_{ij}$ is constructed so that it cancels this contribution:

$$\begin{aligned} &\frac{k}{\tilde{k}} \langle u_j [\tilde{A}_{il}^{-1}(\omega u_l - \langle \omega u_l \rangle)] \rangle \\ &\quad = \frac{k}{\tilde{k}} \tilde{A}_{il}^{-1} \left(\frac{2}{3} \langle \omega \rangle \tilde{k} \tilde{A}_{lj} \right) = \frac{2}{3} k \langle \omega \rangle \delta_{ij}. \end{aligned} \tag{49}$$

It may be observed that in GHT the vanishing of $R_{ij}^{(3)}$ is independent of the properties of A_{ij}. But here the properties of the inverses of A_{ij} and $\tilde{A}_{ij}$ are exploited to effect the cancellation.

[As discussed by Pope and Chen,[14] the occurrence of the inverse A_{ij}^{-1} raises questions of ill conditioning for the limiting case of two-component turbulence, in which an eigenvalue of A_{ij} tends to zero, and hence A_{ij}^{-1} tends to infinity. To avoid such difficulties we replace A_{ij}^{-1} and $\tilde{A}_{ij}^{-1}$ by their "modified determinant" counterparts, defined by Eq. (B3) of Ref. 14. Under normal circumstances this has a negligible effect, but it ensures finite coefficients under all circumstances.]

In summary, the stochastic model for velocity is modified so that, for inhomogeneous flows, the forms of the Reynolds and Reynolds-stress equations are the same as in GHT. No new terms or parameters are added. The resulting stochastic differential equation is Eq. (29), with the drift coefficient given by Eq. (46). In the subsequent calculations G_{ij}^a is taken to be zero, so the only parameter in the model is the constant $C_0 = 3.5$.

IV. JOINT PDF EQUATION

Having obtained stochastic models for $\mathbf{U}^*(t)$ and $\omega^*(t)$, we now write down the corresponding model equation for the one-point Eulerian joint pdf f. Then the equations for the moments $\langle U_i \rangle$, $\langle u_i u_j \rangle$, and $\langle \omega \rangle$ are presented and discussed.

Let $\mathbf{V} = \{V_1, V_2, V_3\}$ and θ be sample-space variables for velocity and relaxation rate, respectively. Then $f(\mathbf{V}, \theta; \mathbf{x}, t)$ is defined to be the joint probability density of the compound event $\{\mathbf{U}(\mathbf{x},t) = \mathbf{V}, \omega(\mathbf{x},t) = \theta\}$.

By standard techniques,[8] the evolution equation for f, obtained from the stochastic models [Eqs. (9), (16), and (29)], is found to be

$$\frac{\partial f}{\partial t} + V_i \frac{\partial f}{\partial x_i} = \frac{1}{\rho} \frac{\partial \langle p \rangle}{\partial x_i} \frac{\partial f}{\partial V_i} - \frac{\partial}{\partial V_i} [f D_i(\mathbf{v})] + \frac{1}{2} C_0 \tilde{k} \theta \frac{\partial^2 f}{\partial V_i \, \partial V_i} + \langle \omega \rangle \frac{\partial}{\partial \theta} \left(f\theta \left\{ S_\omega + C_\chi \left[\ln\left(\frac{\theta}{\langle \omega \rangle}\right) - \left\langle \frac{\omega}{\langle \omega \rangle} \ln\left(\frac{\omega}{\langle \omega \rangle}\right) \right\rangle \right] \right\} \right) - \langle \omega \rangle^2 h \frac{\partial f}{\partial \theta} + C_\chi \langle \omega \rangle \sigma^2 \frac{\partial^2}{\partial \theta^2} (f\theta). \quad (50)$$

Here $D_i(\mathbf{v})$ is the drift term [Eq. (46)] with $\mathbf{u}^*$ replaced by

$$\mathbf{v} \equiv \mathbf{V} - \langle \mathbf{U}(\mathbf{x},t) \rangle, \quad (51)$$

and the coefficients S_ω and h are given by Eqs. (18), (26), and (27).

Before discussing the pdf equation [Eq. (50)], we write down the corresponding model equations for mean continuity; the mean momentum $\langle U_i \rangle$; the Reynolds stresses, $\langle u_i u_j \rangle$; and, the mean relaxation rate $\langle \omega \rangle$. These equations are obtained by multiplying Eq. (50) by 1, V_i, $v_i v_j$, and θ, respectively, and integrating over all $\mathbf{V}$ and θ. The first two results are

$$\frac{\partial \langle U_i \rangle}{\partial x_i} = 0 \quad (52)$$

and

$$\frac{\partial \langle U_i \rangle}{\partial t} + \langle U_j \rangle \frac{\partial \langle U_i \rangle}{\partial x_j} + \frac{\partial}{\partial x_j} \langle u_i u_j \rangle = -\frac{1}{\rho} \frac{\partial \langle p \rangle}{\partial x_i}. \quad (53)$$

The mean continuity equation is, of course, exact, as is the mean momentum equation, save for the neglect of the viscous term. From these two equations we obtain the Poisson equation

$$\frac{\partial^2 \langle p \rangle}{\partial x_i \, \partial x_i} = -\rho \frac{\partial \langle U_i \rangle}{\partial x_j} \frac{\partial \langle U_j \rangle}{\partial x_i} - \rho \frac{\partial^2 \langle u_i u_j \rangle}{\partial x_i \, \partial x_j}, \quad (54)$$

which (with appropriate boundary conditions) determines the mean pressure field.

The modeled Reynolds-stress equation obtained from Eq. (50) is

$$\frac{\partial}{\partial t} \langle u_i u_j \rangle + \langle U_k \rangle \frac{\partial}{\partial x_k} \langle u_i u_j \rangle + \frac{\partial}{\partial x_k} \langle u_i u_j u_k \rangle - \langle u_i u_k \rangle \frac{\partial \langle U_j \rangle}{\partial x_k} - \langle u_j u_k \rangle \frac{\partial \langle U_i \rangle}{\partial x_k} = \langle u_i D_j \rangle + \langle u_j D_i \rangle + C_0 \tilde{k} \langle \omega \rangle \delta_{ij} = -\left(1 + \frac{3}{2} C_0\right) \langle \omega \rangle \left(\langle u_i u_j \rangle - \frac{2}{3} k \delta_{ij} \right) + G^a_{il} \langle u_j u_l \rangle + G^a_{jl} \langle u_i u_l \rangle - \frac{2}{3} \langle \epsilon \rangle \delta_{ij}. \quad (55)$$

It may be observed that (on the left-hand side) the production and transport terms (involving $\langle u_i u_j u_k \rangle$) all stem from the exact term $V_i \, \partial f / \partial x_i$ in the pdf equation, and hence involve no modeling assumptions. As discussed above, the right-hand side of Eq. (55) corresponds to modeled terms for the pressure-rate-of-strain and dissipation.

The modeled equation for $\langle \omega \rangle$ obtained from Eq. (50) is

$$\frac{\partial \langle \omega \rangle}{\partial t} + \langle U_i \rangle \frac{\partial \langle \omega \rangle}{\partial x_i} + \frac{\partial}{\partial x_i} \langle u_i \omega \rangle = -\langle \omega \rangle^2 (S_\omega - h). \quad (56)$$

Returning now to the pdf equation [Eq. (50)], we emphasize that this is a *single*, self-contained, model equation for inhomogeneous turbulent flows: any solution $f(\mathbf{V}, \theta; \mathbf{x}, t)$ *implies* the satisfaction of all moment equations—mean continuity, momentum, etc. Equation (50) is written as a partial differential equation in $\mathbf{V}$-θ-$\mathbf{x}$-t space. But, in fact, it is an integrodifferential equation. For most of the coefficients [e.g., $\langle \omega(\mathbf{x},t) \rangle$ and $\tilde{k}(\mathbf{x},t)$] involve integrals of the joint pdf over $\mathbf{V}$-θ space. And the mean pressure field involves integrals over $\mathbf{x}$ space—i.e., the Green's function solution to the Poisson equation, Eq. (54).

In spite of the onimous appearance of the joint pdf equation, as illustrated in the next section, numerical solutions for inhomogeneous flows can be obtained by Monte Carlo methods.[8,22] In their simplest form, these methods amount to integrating the stochastic equations for $\mathbf{x}^*(t)$, $\mathbf{U}^*(t)$, and $\omega^*(t)$ for a large ensemble of particles. For further details on the Monte Carlo method the reader may consult Refs. 8–12 and 22.

V. CALCULATIONS

In the next three subsections, calculations of three inhomogeneous turbulent flows are presented to demonstrate the satisfactory performance of the joint pdf model. The modeled joint pdf equation has been constructed so that it reverts to the model of Pope and Chen[14] for Gaussian homogeneous turbulence. That model, in turn, yields the same satisfactory Reynolds-stress evolution as the Langevin model of Haworth and Pope.[20,21] Consequently, here it is unnecessary to present again calculations of homogeneous turbulence.

A. Constant-stress wall layer

The first results presented are obtained from a similarity solution of the modeled joint pdf equation, corresponding to the logarithmic law of the wall. In the constant-stress log-law region, the mean velocity and mean dissipation vary strongly with distance from the wall. Hence, as well as being of intrinsic importance, this flow provides a good test of the model's ability to treat strong inhomogeneities in $\langle \mathbf{U} \rangle$, $\langle \epsilon \rangle$, and $\langle \omega \rangle$.

Consider high-Reynolds-number, fully developed channel flow, with the mean flow in the x_1 direction, and with the upper and lower walls being given by $x_2 = H$ and $x_2 = 0$, respectively. Thus all one-point statistics depend on x_2, but are independent of x_1, x_3, and t: the only nonzero mean velocity gradient is $\partial \langle U_1 \rangle / \partial x_2$, which is positive for $x_2 < \frac{1}{2}H$. With the wall shear stress being ρu_τ^2, the viscous length scale is defined by

$$l \equiv \nu / u_\tau. \tag{57}$$

Attention is focused on the constant-stress wall layer, which exists in the region defined by

$$l \ll x_2 \ll H. \tag{58}$$

The statistical properties of this region are well known:[17,18,23] the shear stress is constant,

$$-\langle u_1 u_2 \rangle = u_\tau^2; \tag{59}$$

the mean velocity gradient is

$$\frac{\partial \langle U_1 \rangle}{\partial x_2} = \frac{u_\tau}{\kappa x_2}, \tag{60}$$

where $\kappa = 0.40$ is the von Kármán constant; and the mean dissipation (which balances turbulence production) is

$$\langle \epsilon \rangle = u_\tau^3 / \kappa x_2. \tag{61}$$

Experimental data (see Refs. 17, 18, and 23) also indicate that $\langle u_1^2 \rangle$, $\langle u_2^2 \rangle$, and $\langle u_3^2 \rangle$ are approximately constant in this region.

In view of these known statistical properties, it is natural to seek a similarity solution to the joint pdf equation, in which the one-point joint statistics of

$$\hat{\mathbf{u}}(\mathbf{x},t) \equiv \mathbf{u}(\mathbf{x},t)/u_\tau \tag{62}$$

and

$$\hat{\omega}(\mathbf{x},t) \equiv \omega(\mathbf{x},t) x_2 / u_\tau, \tag{63}$$

are independent of $\mathbf{x}$ and t. That is, defining $\hat{f}(\hat{\mathbf{v}}, \hat{\theta}; \mathbf{x}, t)$ to be the joint pdf of $\hat{\mathbf{u}}$ and $\hat{\omega}$, we seek a solution to the modeled pdf equation corresponding to $\hat{f}$ being independent of $\mathbf{x}$ and t.

In order to derive the evolution equation for $\hat{f}$, we rewrite the joint pdf equation for $f(\mathbf{V}, \theta; x_2, t)$ [Eq. (50)] simply as

$$\frac{\partial f}{\partial t} + V_2 \frac{\partial f}{\partial x_2} = \langle \omega | \mathbf{V}, \theta, x_2 \rangle f R, \tag{64}$$

where the nondimensional quantity $R(\mathbf{V}, \theta, x_2, t)$ embodies all the terms on the right-hand side of Eq. (50). Formally transforming this equation—without any assumption of self-similarity—we obtain the corresponding equation for $\hat{f}(\hat{\mathbf{v}}, \hat{\theta}; \hat{x}_2, t)$:

$$\frac{x_2}{u_\tau}\frac{\partial \hat{f}}{\partial t} + x_2 \hat{v}_2 \frac{\partial \hat{f}}{\partial x_2} - \left\{ \frac{x_2}{u_\tau} \frac{\partial \langle U_1 \rangle}{\partial x_2} \right\} \times \hat{v}_2 \frac{\partial \hat{f}}{\partial \hat{v}_2} + \hat{v}_2 \frac{\partial}{\partial \hat{\theta}} (\hat{f}\hat{\theta}) = \langle \hat{\omega} | \hat{\mathbf{v}}, \hat{\theta}, \hat{x}_2 \rangle \hat{f} R. \tag{65}$$

For a self-similar solution to this equation, the first two terms are zero, since (by definition of such a solution) $\hat{f}$ is independent of t and x_2. With the exception of the quantity in braces, none of the other terms depends on x_2. Consequently, a necessary condition for the existence of a self-similar solution is that the term in braces be constant: that is,

$$\frac{x_2}{u_\tau}\frac{\partial \langle U_1 \rangle}{\partial x_2} = \frac{1}{\kappa}, \tag{66}$$

which is simply the log-law [Eq. (60)].

Thus the self-similar solution was obtained (by Monte Carlo) as the stationary solution of the equation,

$$\frac{\partial \hat{f}}{\partial t} - \frac{\hat{v}_2}{\kappa}\frac{\partial \hat{f}}{\partial \hat{v}} + \hat{v}_2 \frac{\partial}{\partial \hat{\theta}} (\hat{f}\hat{\theta}) = \langle \hat{\omega} | \hat{\mathbf{v}}, \hat{\theta}, \hat{x}_2 \rangle \hat{f} R. \tag{67}$$

For a given model (i.e., given R), a solution to this equation is found for any (reasonable) value of κ. But there is a unique value of κ for which the solution satisfies the consistency condition

$$-\langle \hat{u}_1 \hat{u}_2 \rangle = 1, \tag{68}$$

which stems from Eqs. (59) and (62). Thus, for given R, the value of κ is determined by Eqs. (67) and (68). However, we used these equations a little differently: the value $\kappa = 0.4$ was specified, then the particular value of $C_{\omega 1}$ was determined that yielded a solution to Eq. (67), consistent with Eq. (68)—the result being $C_{\omega 1} = 0.04$. In other words, the value $C_{\omega 1} = 0.04$ was selected to yield $\kappa = 0.4$.

The principal results for the constant-stress wall layer are given in Table I. Compared to the experimental value, the kinetic energy k/u_τ^2 is calculated to within 10%; but the distribution of the energy between the three components is less well calculated. This is a well-known deficiency of Rotta's model that predicts the equality of $\langle u_2^2 \rangle$ and $\langle u_3^2 \rangle$. The kurtosis of u_1 and u_2 are calculated to be very close to the Gaussian value of 3, in accord with the data.

TABLE I. Calculated and measured statistics in the constant-stress wall layer.

	Calculated	Measured
$-\langle u_1 u_2 \rangle / k$	0.29	0.26[a]
k/u_τ^2	3.4	3.8[a]
$\langle u_1^2 \rangle^{1/2}/u_\tau$	1.73	2.07
$\langle u_2^2 \rangle^{1/2}/u_\tau$	1.40	1.0[a]
$\langle u_3^2 \rangle^{1/2}/u_\tau$	1.40	1.55[a]
Kurtosis of u_1	3.04	2.8–3.0[b]
Kurtosis of u_2	3.04	
C_μ	0.075[c]	
σ_ϵ	1.05[d]	

[a] From the data compiled by Phillips[24] at $x_2/l = 100$.
[b] From Durst *et al.*[25]
[c] Evaluated from: $-\langle u_1 u_2 \rangle = C_\mu (k^2/\langle \epsilon \rangle)(\partial \langle U_1 \rangle / \partial x_2)$.
[d] Evaluated from: $-\langle u_2 \epsilon \rangle = (C_\mu/\sigma_\epsilon)(k^2/\langle \epsilon \rangle)(\partial \langle \epsilon \rangle / \partial x_2)$.

The values of the k-ϵ model constants C_μ and σ_ϵ deduced from the calculations can be compared to the standard values of 0.09 and 1.3, respectively.

In summary, the modeled evolution equation for the joint pdf of velocity and dissipation yields a self-similar solution corresponding to the log-law region of the constant-stress wall layer. The model constant $C_{\omega 1}$ is specified to be 0.04, so that the correct value of the von Kármán constant is obtained ($\kappa = 0.4$). The level of agreement between calculated and measured quantities (Table I) is reasonable, and could be improved by incorporating a more sophisticated pressure-strain model, G_{ij}^a.

B. Momentumless wake

The momentumless wake provides a good test of the model's ability to treat turbulent/nonturbulent intermittent regions, in the absence of mean velocity gradients.

Experimentally, plane momentumless wakes have been studied by Townsend,[26] Mobbs,[27] and Cimbala and Park.[28] The flow is created in a wind tunnel by positioning a specially constructed cylinder normal to the uniform flow of nonturbulent air. The cylinder is symmetric about the plane $x_2 = 0$, where x_1, x_2, and x_3 are the streamwise, transverse, and spanwise directions. On the downstream side of the cylinder, air is forced through a slot that runs the length of the cylinder on the plane of symmetry. This air flow forms a plane jet, the flow rate of which is carefully controlled so that the jet's momentum excess exactly equals the momentum deficit of the cylinder's wake.

In the turbulent flow behind the cylinder, the mean axial velocity $\langle U_1 \rangle$ has a maximum on the plane of symmetry, and minima on either side. But the mean velocity profile and the shear stress profile $\langle u_1 u_2 \rangle$ decay more rapidly than do the normal stresses, so that far downstream the mean velocity gradients are negligible, as far as the turbulence is concerned.

In the laboratory frame, this flow is statistically stationary and two dimensional. Far downstream of the cylinder, in a frame moving with the free-stream velocity U_∞, the flow is (to an excellent approximation) statistically one dimensional and evolving. In this frame the momentumless wake appears as a statistically plane patch of turbulence, statistically symmetric about $x_2 = 0$, that spreads into the nonturbulent, quiescent fluid on either side of it. The joint pdf model is applied to this one-dimensional transient problem.

It is natural to question whether or not the flow attains a self-similar state. Let the characteristic velocity scale $u'(t)$ be the rms axial velocity on the plane of symmetry, and let the characteristic length $\Delta(t)$ be the half-width of this rms velocity profile. It is readily shown that necessary conditions for self-similarity are that u' and Δ evolve as

$$u'(t) = u'_0 (t/t_0)^{-a} \tag{69}$$

and

$$\Delta(t) = \Delta_0 (t/t_0)^b, \tag{70}$$

where u'_0 and Δ_0 are the values at time t_0, and the positive constants a and b satisfy

$$a + b = 1. \tag{71}$$

TABLE II. Self-similarity parameters for the momentumless wake.

	a	b	$u't/\Delta$
Townsend[26]	...	0.8	...
Mobbs[27]	...	0.3	...
Cimbala and Park[28]	0.81	0.3	0.47
Cimbala and Park[28] with virtual origin	0.75	0.25	0.44
pdf calculation	0.64	0.36	0.71

In all of the experiments it is found that u' and Δ do indeed vary in time by power laws: the powers a and b are shown in Table II. While Townsend and Mobbs report only b, Cimbala and Park report both a and b, but their sum is not unity [see Eq. (71)]. However, a reexamination of their data reveals that if the virtual origin is accounted for, slightly different values of a and b are obtained that do sum to unity. On this basis, and given the observed collapse of the scaled turbulence intensity profiles, we conclude that the flow does become self-similar. However, for this type of flow, it can be expected that the self-similar state is not unique, but rather is influenced by the initial conditions.[29,30]

The pdf model equations are solved by Monte Carlo as a one-dimensional transient problem, and (almost inevitably) it is found that a self-similar solution is obtained. The calculated spreading-rate exponent $b = 0.36$ is about 20% greater than the experimental values of Mobbs and Cimbala and Park, but much less than the high value $b = 0.8$ obtained by Townsend. The nondimensional measure of the turbulence intensity

$$c \equiv u't/\Delta, \tag{72}$$

is calculated to be about 60% greater than that measured by Cimbala and Park.

The normalized turbulence intensity profiles are shown in Fig. 1. As may be seen, there is excellent agreement between the calculations and the measurements in the self-similar region ($x_1/d \geqslant 5$, say).

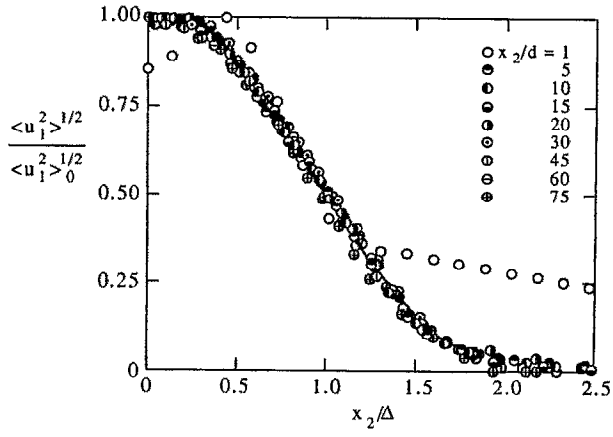

FIG. 1. Profile of axial turbulence intensity for the momentumless wake: $\langle u_1^2 \rangle_0^{1/2}$ is the rms axial velocity on the symmetry plane; Δ is the half-width of the profile; d is the thickness of the cylinder. Solid line: joint pdf calculations; symbols: experimental data.[28] (Figure from Ref. 28, with permission.)

We regard the level of agreement with the data as quite satisfactory. The momentumless wake is an extremely difficult flow to realize, and the constants a, b, and c may well depend on the details of the experiment.

C. Plane mixing layer

We consider the statistically plane, two-dimensional, self-similar mixing layer formed between two uniform streams of different velocities. The dominant flow direction is x_1; the lateral direction is x_2; and the flow is statistically homogeneous in the spanwise direction x_3. The free-stream velocities are U_∞ (at $x_2 = \infty$) and $2U_\infty$ (at $x_2 = -\infty$), so that the velocity ratio is 2, and the velocity difference is $\Delta U = U_\infty$. At large axial distances the flow spreads linearly and is self-similar.[17] Consequently, statistics of $\mathbf{U}(\mathbf{x},t)/\Delta U$ depend only on x_2/x_1 [where $(x_1,x_2) = (0,0)$ is the virtual origin of the mixing layer]. Lang[31] provides experimental data on this flow.

The joint pdf equations are solved by a Monte Carlo method, which marches in the axial direction until the self-similar state has been attained. As a test of the model, this flow combines features found in the two flows considered above. There is mean shear and inhomogeneity in the Reynolds stresses and dissipation; and, on both sides of the flow, there are intermittent turbulent/nonturbulent regions.

Figure 2 shows the calculated mean velocity profile compared to Lang's experimental data.[31] The observed good agreement indicates, not only that the profile shape is well calculated, but that the spreading rate is accurate as well. The spreading rate can be defined as Δ/x_1, where the width of the layer Δ is defined as the distance in x_2 between the points where the mean velocity is $1.1U_\infty$ and $1.9U_\infty$. The experimental[31] and calculated values of Δ/x_1 are 0.050 and 0.047, respectively.

The agreement of the spreading rates is by no means inevitable. In this type of flow, the calculated spreading rate is sensitive to the specified constants $C_{\omega 1}$ and $C_{\omega 2}$ in the ω equation. The constant $C_{\omega 1}$ is specified to be 0.04—about half that suggested by the k-ϵ model—in order to yield the correct value of the von Kármán constant. It is reassuring to observe, therefore, that the same value of $C_{\omega 1}$ also leads to an accurate calculation of the spreading rate for the mixing layer.

Figure 3 shows the calculated rms lateral velocity profile, which agrees quite well with the data. The level of agreement for the axial velocity (not shown) is comparable.

Of course the joint pdf calculations produce vastly more information than is contained in the first and second moment profiles presented above. The next three figures illustrate this point.

Figure 4 is a scatter plot of the axial velocity and lateral position. In the Monte Carlo calculation, at each axial location (x_1), the joint pdf is represented by an ensemble of N particles ($N \approx 50\,000$). Each particle has a lateral position x_2^*, a velocity $\mathbf{U}^*$, and a relaxation rate ω^*. Figure 4 consists of the ($\approx 10\,000$) points with coordinates $(x_2^*/x_1,\ U_1^*/\Delta U)$ corresponding to one-fifth of the particles (selected at random).

At large and small values of x_2^*/x_1, the points are dense at $U_1^*/\Delta U = 1$ and 2, respectively, and so appear as horizontal straight lines. These points correspond to fluid with the free-stream velocity. At the center of the layer (e.g., $x_2^*/x_1 = 0$), the points are broadly scattered in $U_1^*/\Delta U$, indicative of turbulent fluctuations with rms of order 0.2. Toward the edges of the layer, biomodal behavior is evident: with increasing distance from the layer, a band of points tends to the free-stream velocity, while other points exhibit fluctuations of order 0.1, but with decreasing probability. This reflects the turbulent/nonturbulent nature of these regions.

The intermittent nature of the edges of the mixing layer is yet more evident in Fig. 5, which is a scatter plot of relaxation rate and lateral position. The relaxation rate is normalized by its maximum mean value $\langle\omega\rangle_{\max}$ (at the axial location considered) and is shown on a logarithmic scale. At the edges of the layer the bimodal nature of ω^* is clear: there is a diffuse band of points centered around $\omega^* \sim 0.3\langle\omega\rangle_{\max}$, with a second denser band with ω^* values two or three orders of magnitude less. These bands correspond to turbulent and nonturbulent fluid, respectively. In the center of the layer, $\mu_{1/2}$ [Eq. (23)] is observed to be very close to its Gaussian value, but it tends to zero at the edges indicative of a bimodal

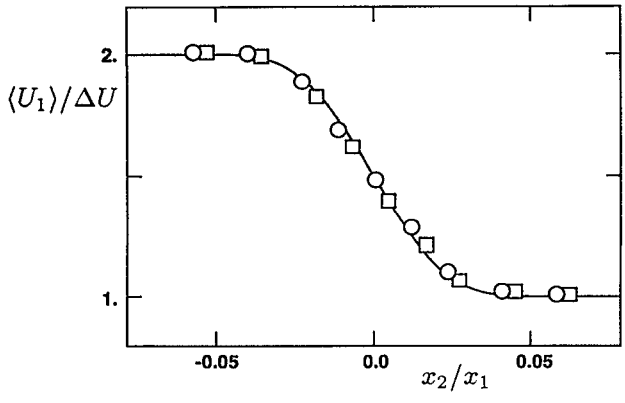

FIG. 2. Mean axial velocity profile for the self-similar plane mixing layer: line—joint pdf calculations; symbols—experimental data of Lang.[31]

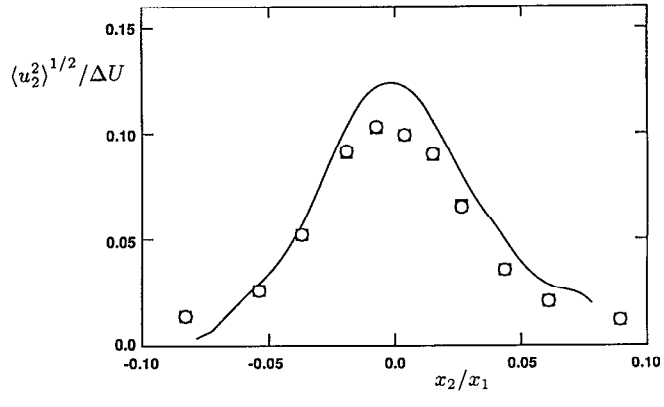

FIG. 3. rms lateral velocity profile for the self-similar plane mixing layer: line—joint pdf calculations; symbols—experimental data of Lang.[31]

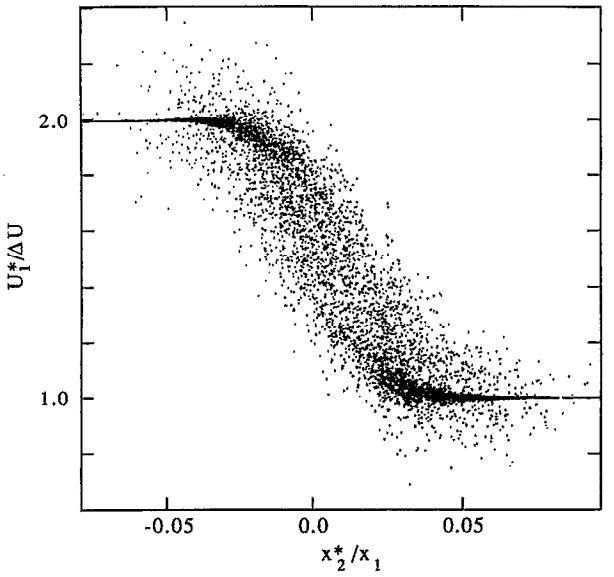

FIG. 4. Scatter plot of axial velocity and lateral position from joint pdf calculations of the self-similar plane mixing layer.

(nonlognormal) pdf of ω in the intermittent region.

The model developed here has been presented in the context of the one-point one-time Eulerian joint pdf of $\mathbf{U}$ and ω. But the stochastic models used also provide closure to the multitime Lagrangian pdf equations. Figure 6 shows some Lagrangian information extracted from the Monte Carlo calculations—namely, the fluid particle paths of five particles whose initial positions are selected at random near the center of the layer, once it has become self-similar. It may be observed that several of these trajectories traverse the layer monotonically, and that the trajectories are devoid of high wave number fluctuations. From this we conclude that the motion implied by the model is consistent with the large-scale coherent motions observed experimentally in mixing layers; and, conversely, it does not resemble the small-scale random motion associated with diffusion models.

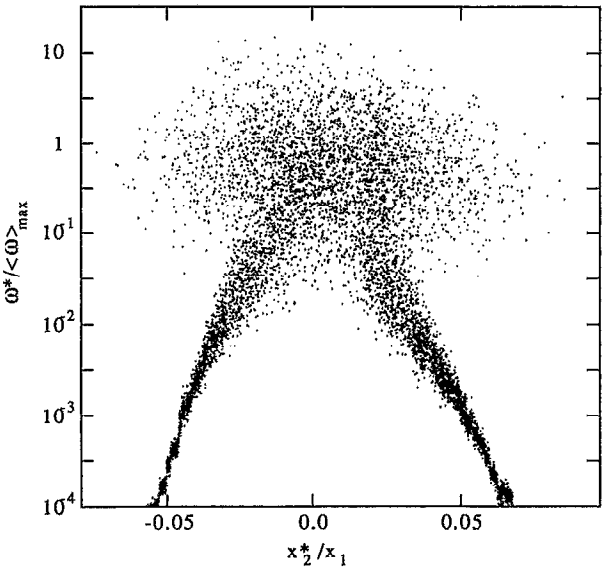

FIG. 5. Scatter plot of relaxation rate and lateral position from joint pdf calculations of the self-similar plane mixing layer: ω^* is normalized by the maximum value of $\langle\omega\rangle$ across the profile.

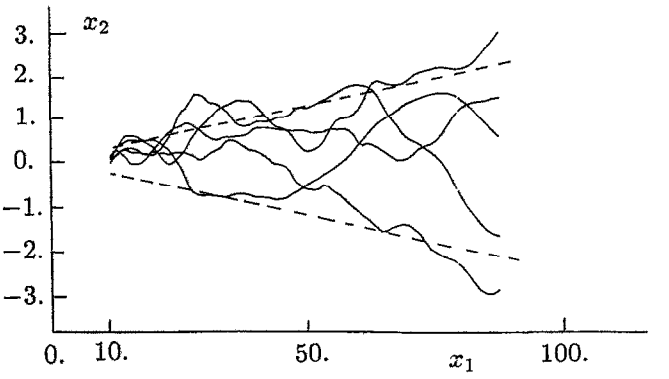

FIG. 6. Fluid particle paths in the plane mixing layer according to the stochastic models: x_1 and x_2 have arbitrary units. The dashed lines show the nominal edges of the layer, where the mean velocity differs from the free-stream velocity by 10% of the velocity difference.

VI. SUMMARY AND CONCLUSION

The velocity-dissipation joint pdf model of Pope and Chen[14] has been extended to inhomogeneous flows. The model is based on stochastic processes for the velocity $\mathbf{U}^*(t)$ and relaxation rate $\omega^*(t)$ [Eq. (10)] following fluid particles.

The principal modification to the stochastic differential equation for $\omega^*(t)$ is the addition of an extra drift term that allows $\omega^*(t)$ to increase from zero. For Gaussian homogeneous turbulence, $\mathbf{U}^*(t)$ and $\omega^*(t)$ are statistically independent. For inhomogeneous flows, the stochastic differential equation for velocity is modified so as to retain the same basic properties, even though $\mathbf{U}^*(t)$ and $\omega^*(t)$ are not independent.

From the coupled stochastic differential equations for $\mathbf{x}^*(t)$, $\mathbf{U}^*(t)$, and $\omega^*(t)$, several closed model pdf equations can be derived—both Eulerian and Lagrangian. In particular, the one-point one-time Eulerian joint pdf of $\mathbf{U}(\mathbf{x},t)$ and $\omega(\mathbf{x},t)$ is presented as Eq. (50). This is a single, closed model equation for inhomogeneous turbulent flows.

The performance of the model has been demonstrated by calculations of three different inhomogeneous flows. In each case the modeled pdf equation is solved numerically by a Monte Carlo method. This consists, essentially, of solving the stochastic differential equations for an ensemble of (typically 50 000) particles.

A self-similarity solution is obtained corresponding to the log-law region of a turbulent boundary layer. With a model constant selected to obtain the correct value of the von Kármán constant ($C_{\omega 1} = 0.04$, $\kappa = 0.4$), other numerical characteristics are calculated with reasonable accuracy (see Table I).

The calculations of the momentumless wake demonstrate the ability of the model to describe turbulent/nonturbulent regions, without explicit modeling of intermittency. Particle paths for the mixing layer (Fig. 6) illustrate that the

model is consistent with large-scale organized motions.

The model described here can readily be extended to include scalars representing the fluid composition.[2] Consequently it can be applied to problems of mixing and reaction in turbulent flows.

ACKNOWLEDGMENTS

This work is supported in part by contract "Combustion Design Model Evaluation" (F33615-87-C-2821) from the U.S. Air Force Wright Aeronautical Laboratories to Allison Gas Turbine Division, General Motors Corporation, and, in part, by the Grant No. CBT-8814655 from the National Science Foundation.

[1] J. L. Lumley, in *Whither Turbulence? Turbulence at the Crossroads* (Springer-Verlag, Berlin, 1990).
[2] S. B. Pope, in *23rd International Symposium on Combustion* (The Combustion Institute, Pittsburgh, PA, in press).
[3] W. P. Jones and B. E. Launder, Int. J. Heat Mass Transfer **15**, 301 (1972).
[4] B. E. Launder and D. B. Spalding, *Mathematical Models of Turbulence* (Academic, New York, 1972).
[5] B. E. Launder, in Ref. 1, p. 439.
[6] C. G. Speziale, Annu. Rev. Fluid Mech. **23**, 107 (1991).
[7] J. L. Lumley, J. Appl. Mech. **50**, 1097 (1983).
[8] S. B. Pope, Prog. Energy Combust. Sci. **11**, 119 (1985).
[9] M. S. Anand, S. B. Pope, and H. C. Mongia, in *Turbulent Reactive Flows*, Lecture Notes in Engineering (Springer-Verlag, Berlin, 1989), Vol. 40, p. 672.
[10] M. S. Anand, S. B. Pope, and H. C. Mongia, in *CFD Symposium on Aeropropulusion* (NASA Lewis, Cleveland, OH, 1990).
[11] D. C. Haworth and S. H. El Tahry, in *7th Symposium on Turbulent Shear Flows* (Stanford University, Stanford, CA, 1989), p. 13.1.
[12] D. C. Haworth and S. H. El Tahry, AIAA J. **29**, 208 (1991).
[13] S. B. Pope, Phys. Fluids **24**, 588 (1981).
[14] S. B. Pope and Y. L. Chen, Phys. Fluids A **2**, 1437 (1990).
[15] C. W. Gardiner, *Handbook of Stochastic Methods* (Springer-Verlag, Berlin, 1985).
[16] O. M. Phillips, J. Fluid Mech. **51**, 97 (1972).
[17] A. A. Townsend, *The Structure of Turbulent Shear Flow*, 2nd ed. (Cambridge U.P., Cambridge, 1976).
[18] A. S. Monin and A. M. Yaglom, *Statistical Fluid Mechanics Vol. 1* (MIT Press, Cambridge, MA, 1971).
[19] J. C. Rotta, Z. Phys. **129**, 547 (1951).
[20] D. C. Haworth and S. B. Pope, Phys. Fluids **29**, 387 (1986).
[21] D. C. Haworth and S. B. Pope, Phys. Fluids **30**, 1026 (1987).
[22] D. C. Haworth and S. B. Pope, J. Comput. Phys. **72**, 311 (1987).
[23] J. O. Hinze, *Turbulence* (McGraw-Hill, New York, 1975).
[24] W. R. C. Phillips, Phys. Fluids **30**, 23, 54 (1987).
[25] F. Durst, J. Jovanovic, and Lj. Kanevce, in *Turbulent Shear Flows 5*, (Springer-Verlag, Berlin, 1987).
[26] A. A. Townsend, *The Structure of Turbulent Shear Flows*, 1st ed. (Cambridge U.P., Cambridge, 1956).
[27] F. R. Mobbs, J. Fluid Mech. **33**, 227 (1968).
[28] J. M. Cimbala and W. J. Park, J. Fluid Mech. **213**, 479 (1990).
[29] I. Wygnanski, F. Champagne, and B. Marasli, J. Fluid Mech. **168**, 31 (1986).
[30] W. K. George, in *Advances in Turbulence*, edited by W. K. George and R. Arndt (Hemisphere, New York, 1989).
[31] D. B. Lang, Ph.D. thesis, California Institute of Technology, 1985.